A Conceptual Model for the Reflection Measurements of a Vector Network Analyzer System and its Practical Application

Nikolitsa I. Yannopoulou and Petros E. Zimourtopoulos

Antennas Research Group, Austria, EU - www.op4.eu

Abstract

We present the gradual building of our conceptual model for the reflection measurements of a VNA Vector Network Analyzer System. In this way, we reveal the fundamental idea behind this kind of measurements and prepare the studier for a deeper comprehension of this subject. Moreover, since this abstract model is exclusively based on technical specifications supplied by the manufacturers of system components, it is directly applicable in practice. To demonstrate this fact, we use a specific VNA System to compute and draw both the frequency dependent systematic error parameters of it and of the reflection coefficient and input impedance of a particular antenna we constructed and measured by using it.

Keywords

Microwave measurements, network analyzer, differential error region, differential error interval, S-parameters, calibration, antenna measurements, reflection measurements

Introduction

The measurement system of our conventional Vector Network Analyzer (VNA) with two measurement ports under Automated control via HPIB with the developed by us application [ANALYZE] and with an external signal generator to ensure the frequency stability through Phase-Locked Loop (PLL) characteristic is presented in Fig. 1. The well-known set-up of the reflection coefficient measurements of a Device Under Test (DUT) by using such a VNA is shown in detail in Fig. 2. The relation between the reflection coefficient of the DUT and its measured value can be mathematically described by the commonly accepted One Port Measurement Error Model

[1]. We thought that the necessarily abstract nature of this model obscures the relations between the involved quantities making difficult any further study. Although it seems that numerous articles have been appeared which describe a number of approaches to this measurement theory (e.g. [2] - [6]), these do not satisfy our demand for clearness. Therefore, we decided to attempt a different one overall examination of the measurement process in order to found our further research.

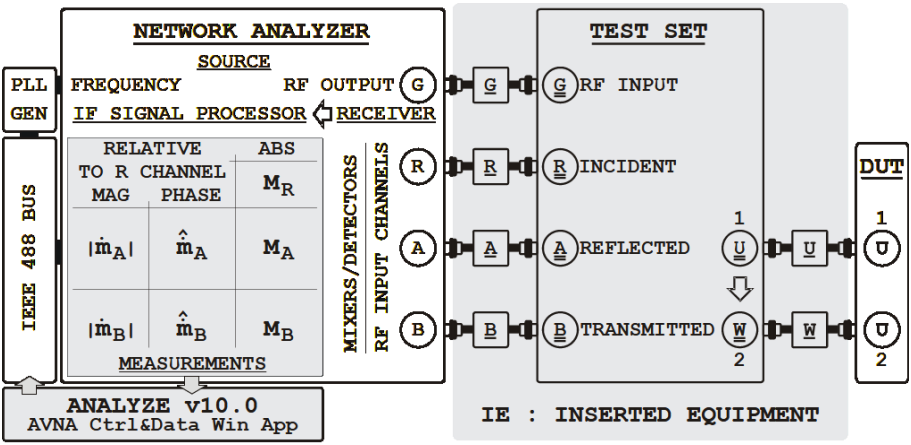

Fig. 1: Automated VNA measurement system

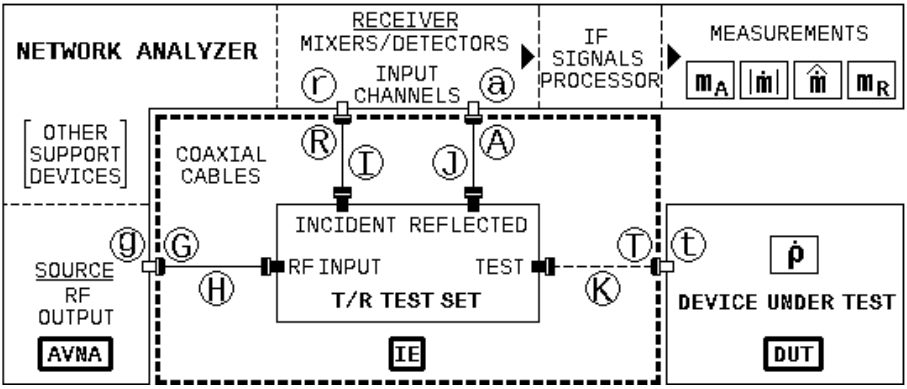

Fig. 2: Reflection measurements set-up

Analysis

We start our analysis considering that the measuring system consists of three distinct but interconnected parts accordingly to the amount of the available technical information.

The first part is active and contains the VNA itself plus any other supporting devices. The essential characteristic of this part is the great requirement for a complete analysis. Because of this complication, we have to base our study on overall external technical characteristics supplied by the manufacturer. In this way the VNA part can be described by a mathematical model of a rather theoretical nature.

The second part is the DUT itself. A model for this device consists of a single set definition for the considered reflection coefficient values.

The third part is passive and stands between the VNA and the DUT. We call this part "Inserted Equipment" (IE). A dashed bold line in Fig. 2 surrounds the IE part including the Transmission/Reflection Test Set (T/R) and the Coaxial Cables H, I, J and K. The K cable is added for the slightly more general case of a distanced DUT. The essential of the IE part is that it is capable of analysis based on technical characteristics supplied by the manufacturer.

In this way the IE part can be described by a mathematical model of a rather constructional nature. The model consists of an assembly of sets and functions. The three IE ports G, R, A are directly connected to the VNA ports g, r and a respectively and the fourth one T is connected to DUT port t. In these ports the models of the three parts have to interface each other by a set of mathematical relations.

Generally, the VNA source impresses a voltage to IE port G, which in the presence of the DUT reflection coefficient produces a pair of voltages to the VNA receiver ports, a and r.

After mixing and detecting the signals processor produces a quadruplet of measurements for the absolute amplitudes of the input signals and the amplitude and phase of their ratio. The existence of another input port B is connected to transmission measurements, therefore it is not involved here.

Theory

Let Z_0 be the system's characteristic impedance which is a constant positive real number, so we have

$$\boxed{Z_0 \in \mathbb{R}_+} \quad (1)$$

and from this

$$Y_0 \equiv \frac{1}{Z_0} \in \mathbb{R}_+ \quad (2)$$

Z_0 is the first of our model constants. We consider RMS values in the phasor notation for the involved quantities. In order to keep track of the used symbols we declare here the used notation: A dot over symbol represent complex quantity, a prime corresponds to the real part and a double prime to the imaginary part. Bold normal letters are used to define sets while bold italic define functions.

At each port x of the measurement system of Fig. 2, where

$$x = g, a, r, t, G, A, R, T \quad (3)$$

we consider the levels of the "normalized" [7] incoming $\dot{a}_x$ and outgoing $\dot{b}_x$ wave values at this x port, as they are defined by the relations

$$\dot{a}_x = \frac{\dot{V}_x + Z_0 \dot{I}_x}{2\sqrt{Z_0}}, \quad \dot{b}_x = \frac{\dot{V}_x - Z_0 \dot{I}_x}{2\sqrt{Z_0}} \quad (4)$$

where

$$\dot{a}_x = a_x' + i\, a_x'', \quad \dot{b}_x = b_x' + i\, b_x''$$

so that the following relations are valid:

$$\dot{V}_x = \sqrt{Z_0}(\dot{a}_x + \dot{b}_x), \quad (5a)$$

$$\dot{I}_x = \sqrt{Y_0}(\dot{a}_x - \dot{b}_x) \quad (5b)$$

$$\dot{V}_{a_x} \equiv \sqrt{Z_0}\dot{a}_x, \quad \dot{V}_{b_x} \equiv \sqrt{Z_0}\dot{b}_x, \quad (6a)$$

$$\dot{I}_{a_x} \equiv \sqrt{Y_0}\dot{a}_x, \quad \dot{I}_{b_x} \equiv -\sqrt{Y_0}\dot{b}_x \quad (6b)$$

$$\dot{V}_x = \dot{V}_{a_x} + \dot{V}_{b_x}, \quad \dot{I}_x = \dot{I}_{a_x} + \dot{I}_{b_x} \quad (7)$$

$$\dot{P}_{a_x} \equiv \dot{V}_{a_x} \overset{*}{\dot{I}}_{a_x} = a_x^2 = P_{a_x}' \geq 0, \quad (8a)$$

$$P_{a_x}'' = 0 \quad (8b)$$

$$\dot{P}_{b_x} \equiv \dot{V}_{b_x} \overset{*}{\dot{I}}_{b_x} = -b_x^2 = P_{b_x}' \leq 0, \quad (9a)$$

$$P_{b_x}'' = 0 \quad (9b)$$

$$\dot{P}_x = (\dot{V}_x \overset{*}{\dot{I}}_x) = (\dot{a}_x + \dot{b}_x)(\dot{a}_x - \dot{b}_x)^* =$$

$$= (|\dot{a}_x|^2 - |\dot{b}_x|^2) - 2i(\dot{a}_x \overset{*}{\dot{b}}_x)'' \quad (10)$$

$$P_x' \equiv (\dot{P}_x)' = (\dot{V}_x \overset{*}{\dot{I}}_x)' = |\dot{a}_x|^2 - |\dot{b}_x|^2 =$$

$$= a_x^2 - b_x^2 = P_{a_x}' + P_{b_x}' \quad (11)$$

$$\dot{\rho}_x \equiv \dot{\rho}_{V_x} \equiv \frac{\dot{V}_{b_x}}{\dot{V}_{a_x}} = \frac{\dot{b}_x}{\dot{a}_x} \quad (12a)$$

$$\dot{\rho}_{I_x} \equiv \frac{\dot{I}_{b_x}}{\dot{I}_{a_x}} = -\frac{\dot{b}_x}{\dot{a}_x} = -\dot{\rho}_x \quad (12b)$$

$$\dot{V}_{a_x} \neq 0, \quad \dot{a}_x \neq 0 \quad (12c)$$

and especially for an one port only passive network

$$0 \le P' = a^2 - b^2 = a^2\left(1 - \frac{b^2}{a^2}\right) \Rightarrow$$

$$\Rightarrow 0 \le 1 - \frac{b^2}{a^2} = 1 - \rho^2 = (1+\rho)(1-\rho)$$

$$\Rightarrow 0 \le \rho^2 \le 1 \Rightarrow 0 \le \rho \le 1 \qquad (13)$$

so that for all one port passive networks or loads we have

$$\boxed{\dot{\boldsymbol{\rho}} \equiv \{\dot{\rho} \mid 0 \le |\dot{\rho}| \le 1 \subset \dot{\mathbb{C}}} \qquad (14)$$

We consider this set as one of the involved sets in our model, while

$$\frac{\dot{P}_b}{\dot{P}_a} = \frac{P_b'}{P_a'} = \frac{\dot{V}_b \overset{*}{\dot{I}}_b}{\dot{V}_a \overset{*}{\dot{I}}_a} = \left(\frac{\dot{V}_b}{\dot{V}_a}\right)\left(\frac{\overset{*}{\dot{I}}_b}{\overset{*}{\dot{I}}_a}\right) =$$

$$= \dot{\rho}_V \overset{*}{\dot{\rho}}_I = \dot{\rho}_V\left(-\overset{*}{\dot{\rho}}_V\right) =$$

$$= -|\dot{\rho}_V|^2 = -\frac{b^2}{a^2} = -\rho^2 \qquad (15)$$

and in each interconnection of the ports x (g, a, r, t), and X (G, A, R, T), we have the interface relations:

$$\dot{V}_X = \dot{V}_x, \quad \dot{I}_X = -\dot{I}_x,$$

$$\dot{a}_X = \dot{b}_x, \quad \dot{b}_X = \dot{a}_x, \qquad (16)$$

$$\dot{P}_X = -\dot{P}_x, \quad P_X' = -P_x' \quad P_X'' = -P_x''$$

A. The VNA

The first part can be described from the available VNA technical specifications, which can be qualified by properly defined sets.

A1. Frequency range

If f_m and f_M are the minimum and maximum operating frequencies respectively then

$$\boxed{\mathbf{f} \equiv [f_m, f_M] = \{f \mid 0 < f_m \le f \le f_M\} \subset \mathbb{R}_+} \qquad (17)$$

We consider the f as the first independent variable of our model, with values in the above real interval.

A2. The Source

We interpret the technical characteristics for the output power by the equivalence shown in Fig. 3 under the ideal conditions. We will use the VNA source to feed passive loads exclusively.

After the above relations we have obviously from Fig. 3 at ports g, G:

$$\dot{b}_g = \dot{a}_G = \dot{\rho}_S \dot{a}_g + \frac{(1-\dot{\rho}_S)}{2}\dot{e}_S =$$

$$= \dot{\rho}_S \dot{b}_G + \frac{(1-\dot{\rho}_S)}{2}\dot{e}_S, \ \dot{e}_S \equiv \frac{\dot{E}_S}{\sqrt{Z_0}} \qquad (18)$$

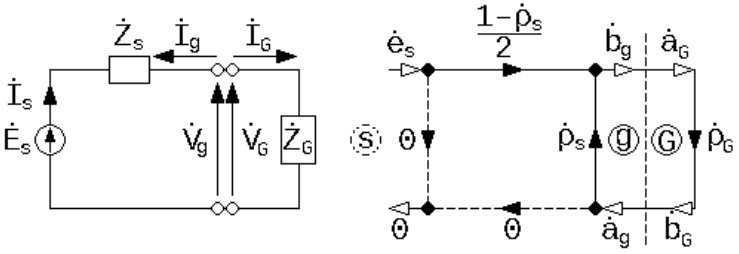

Fig. 3: One port S-parameter flow graph equivalent for a voltage source

for every source reflection coefficient $\dot{\rho}_S \in \dot{\boldsymbol{\rho}}_S$ and

$$\dot{\boldsymbol{\rho}}_S \equiv \{\dot{\rho} \,|\, (\dot{\rho} \in \dot{\boldsymbol{\rho}}) \,\&\, (\rho \neq 1)\} \subset \dot{\boldsymbol{\rho}} \quad (19)$$

which obviously in general can contain every reflection coefficient value except of an open circuit. By rearranging (18) taking into account that

$\dot{b}_G = \dot{\rho}_G \dot{a}_G$ we have

$$2(1 - \dot{\rho}_S \dot{\rho}_G)\dot{a}_g = (1 - \dot{\rho}_S)\dot{e}_S \quad (20)$$

$$\dot{\rho}_G \in \dot{\boldsymbol{\rho}}_G \equiv \{\dot{\rho} \,|\, (\dot{\rho} \in \dot{\boldsymbol{\rho}}) \,\&\, (\rho < 1)\} \subset \dot{\boldsymbol{\rho}} \quad (21)$$

The last one can be used to define the function:

$$\boldsymbol{e}_S : \dot{\boldsymbol{\rho}}_S \times \dot{\boldsymbol{\rho}}_G \times \mathbb{R}_+ \rightarrow \mathbb{R}_+ ; \quad (22)$$

$$\forall \dot{\rho}_S \in \dot{\boldsymbol{\rho}}_S,\ \forall \dot{\rho}_G \in \dot{\boldsymbol{\rho}}_G,\ \forall P \exists ! P_G' \in \mathbb{R}_+$$

$$e_S(\dot{\rho}_S, \dot{\rho}_G, P_G') = \frac{2\,|1 - \dot{\rho}_S \dot{\rho}_G|}{\sqrt{(1-\rho_G^2)}\,|1 - \dot{\rho}_S|}\sqrt{P_G'}$$

As we described the VNA's source as a voltage source in the way shown in Fig. 3 and equivalently by the one-port S-parameter flow graph, it is possible to include a quantitative description of the RF source level in dBm by the well known relation

$$\widetilde{P}[\mathrm{dBm}] \equiv 10 \log \frac{P[\mathrm{W}]}{10^{-3}[\mathrm{W}]} \quad (23)$$

via the constantly real average power P_S to port S which includes a constant amplitude incoming without any outgoing wave. We consider the $\widetilde{P}_0[\mathrm{dBm}]$ as the second independent variable of the model from which the value of the voltage source can be defined by the interval:

$$\boxed{\widetilde{\boldsymbol{P}}_0 \equiv [\widetilde{P}_{0_m}, \widetilde{P}_{0_M}] \subset \mathbb{R}_+} \quad (24)$$

where $\widetilde{P}_{0_m}, \widetilde{P}_{0_M}$ are the minimum and maximum output power levels in dBm as they are defined in manufacturer's characteristics, where as usual we have in general:

$$P_0 = 10^{-3}10^{\frac{\widetilde{P}_0}{10}} \quad (25)$$

Then we can define the functions

$$\boldsymbol{e}_0 : \widetilde{\mathbf{P}}_0 \to \mathbb{R}_+ ; \forall \widetilde{P}_0 \in \widetilde{\mathbf{P}}_0, \exists ! e_0 \in \mathbb{R}_+,$$

$$e_0 \equiv e_0(\widetilde{P}_o) \equiv e_S(\dot{\rho}_S = 0, \dot{\rho}_G = 0,$$

$$P_G^{'} = P_0 = 10^{-3}10^{\frac{\widetilde{P}_0}{10}}) =$$

$$= 2\sqrt{10^{-3}}10^{\frac{\widetilde{P}_0}{20}} \quad (26)$$

$$\boldsymbol{E}_0 : \widetilde{\mathbf{P}}_0 \to \mathbb{R}_+ ; \forall \widetilde{P}_0 \in \widetilde{\mathbf{P}}_0, \exists ! E_0 \in \mathbb{R}_+,$$

$$E_0 \equiv E_0(\widetilde{P}_0) \equiv \sqrt{Z_0}e_0(\widetilde{P}_0) =$$

$$= 2\sqrt{10^{-3}Z_0}10^{\frac{\widetilde{P}_0}{20}} \quad (27)$$

$$\mathbf{E}_0 \equiv \boldsymbol{E}_0[\widetilde{P}_0] \quad (28)$$

$$\hat{\mathbf{E}}_0 \equiv (-\pi, \pi] \quad (29)$$

$$\dot{\boldsymbol{E}}_0 : \widetilde{\mathbf{P}}_0 \times (-\pi, \pi] \to \mathbb{C} \quad (30)$$

$$\dot{\mathbf{E}}_0 \equiv \{\dot{E}_0 \equiv E_0 e^{i\hat{E}_0} \mid$$

$$\mid (E_0 \in \mathbf{E}_0) \,\&\, (\hat{E}_0 \in \hat{\mathbf{E}}_0)\} \quad (31)$$

$$\dot{\boldsymbol{e}}_0 : \widetilde{\mathbf{P}}_0 \times (-\pi, \pi] \to \mathbb{C};$$

$$\dot{\boldsymbol{e}}_0 \equiv \frac{1}{Z_0}\dot{\boldsymbol{E}}_0 \quad (32)$$

and another one function for the impressed voltage source so that

$$\mathbf{e}_g \equiv [e_{g_m}, e_{g_M}] = \quad (33)$$

$$\{e_g \equiv |\dot{e}_g| : 0 < e_{g_m} \le e_g \le e_{g_M}\} \subset \mathbb{R}_+$$

We consider an undetermined but constant value for the phase $\hat{E}_g$ of the voltage source and finally

$$\dot{\mathbf{e}}_g \equiv \{\dot{e}_g \equiv e_g e^{i\hat{e}_g} \mid$$

$$\mid (e_g \in \mathbf{e}_g) \,\&\, \hat{e}_g \in (-\pi, \pi]\} \quad (34)$$

For passive load connected to port G, with a reflection coefficient $\dot{\rho}_G$, we have, as before, a voltage drop

$$\dot{\mathbf{e}}_G \equiv \{\dot{e}_G \equiv e_G e^{i\hat{e}_G} \mid$$

$$\mid (e_G \in \mathbf{e}_G) \,\&\, \hat{e}_G \in (-\pi, \pi]\} \quad (35)$$

A3. The Receiver Inputs

We accept that do not take into account any dependence of the output voltage from the frequency because it is always possible to adjust the receiver inputs independently in a way that always guarantees that the output voltage lies between the above values. The frequency f and the output voltage levels E are the VNA's independent variables. If we admit, for simplicity, that the input channels are independent but they have identical characteristics for the maximum permissible input level V_{i_M} and the

minimum detectable level above some noise floor V_{i_m} then, as above, we have:

$$\mathbf{V}_i \equiv [V_{i_m}, V_{i_M}] = \{V_i \equiv |\dot{V}_i| : 0 < V_{i_m} \le V_i \le V_{i_M}\} \subset \mathbb{R}_+ \quad (36)$$

$$\hat{\mathbf{V}}_i \equiv (-\pi, \pi] = \{\hat{V}_i \equiv \sphericalangle \dot{V}_i \mid -\pi < \hat{V}_i \le \pi\} \subset \mathbb{R} \quad (37)$$

$$\dot{\mathbf{V}}_i \equiv \{\dot{V}_i \equiv V_i e^{i\hat{V}_i} \mid \mid (V_i \in \mathbf{V}_i) \,\&\, (\hat{V}_i \in \hat{\mathbf{V}}_i)\} \subset \mathbb{C} \quad (38)$$

so at the input ports a and r

$$\mathbf{V}_a = \mathbf{V}_r = \mathbf{V}_i \quad (39)$$

$$\hat{\mathbf{V}}_a = \hat{\mathbf{V}}_r = \hat{\mathbf{V}}_i \quad (40)$$

$$\dot{\mathbf{V}}_a = \dot{\mathbf{V}}_r = \dot{\mathbf{V}}_i \quad (41)$$

$$\tilde{\mathbf{P}}_i \equiv [\tilde{P}_{i_m}, \tilde{P}_{i_M}] \subset \mathbb{R}_+ \quad (42)$$

A4. The measurement ranges

A4a. Magnitude

The measurements concern the magnitude of the input signals at A, R ports and the magnitude and phase of their ratio. In the same manner as above, we have for the magnitude

$$\tilde{\mathbf{M}}_i \equiv [\tilde{M}_{i_m}, \tilde{M}_{i_M}] = \{\tilde{M}_i \mid 0 < \tilde{M}_{i_m} \le \tilde{M}_i \le \tilde{M}_{i_M}\} \subset \mathbb{R}_+ \quad (43)$$

$$\tilde{\mathbf{M}}_a = \tilde{\mathbf{M}}_r = \tilde{\mathbf{M}}_i \quad (44)$$

and for the ratio

$$\tilde{\mathbf{m}}_i \equiv [\tilde{m}_m, \tilde{m}_M] = \{\tilde{m} \mid 0 < \tilde{m}_m \le \tilde{m} \le \tilde{m}_M\} \subset \mathbb{R}_+ \quad (45)$$

$$\hat{\mathbf{m}} \equiv (-\pi, \pi] = \{\hat{m} \equiv \sphericalangle \dot{m} \mid -\pi < \hat{m} \le \pi\} \subset \mathbb{R} \quad (46)$$

hence

$$\dot{\mathbf{m}} \equiv \{\dot{m} \equiv 10^{\frac{\tilde{m}}{20}} e^{i\hat{m}} \mid \mid (\tilde{m} \in \tilde{\mathbf{m}}) \,\&\, (\hat{m} \in \hat{\mathbf{m}})\} \subset \mathbb{C} \quad (47)$$

A5. Measurement operation

A5a. Input channel Magnitude measurement

If we consider for each input channel A, R the functions

$$\boldsymbol{M}_A : \mathbf{f} \times \mathbf{V}_A \to \mathbf{M}_A \quad (48)$$

$$\boldsymbol{M}_R : \mathbf{f} \times \mathbf{V}_R \to \mathbf{M}_R \quad (49)$$

but

$$\dot{\mathbf{V}}_A = \dot{\mathbf{V}}_R = \dot{\mathbf{V}}_i \quad (50)$$

$$\mathbf{M}_A = \mathbf{M}_R = \mathbf{M}_i \quad (51)$$

and if

$$\boldsymbol{M}_i : \mathbf{f} \times \mathbf{V}_i \to \mathbf{M}_i \quad (52)$$

such that

$$\boldsymbol{M}_A = \boldsymbol{M}_R = \boldsymbol{M}_i \tag{53}$$

obviously

$$V_i^2 = Z_0(a_i^2 + b_i^2 + 2(\dot{a}_i \overset{*}{\dot{b}_i})') = \\ = Z_0(1 + \rho_i^2 + 2\dot{\rho}_i')a_i^2 \tag{54}$$

The ρ_i has a value rather far away from unit, so that

$$0 < 1 - \rho_i^2 \tag{55}$$

$$-\dot{\rho}_i' \le |\dot{\rho}_i'| \le \rho_i < 1 \Rightarrow 1 + \rho_i^2 + 2\dot{\rho}_i' = \\ = (1 + \dot{\rho}_i')^2 + \dot{\rho}_i''^2 > 0 \tag{56}$$

$$\dot{P}_i' \equiv (\dot{V}_i \overset{*}{\dot{I}_i})' = a_i^2 - b_i^2 = (1 - \rho_i^2)\, a_i^2 = \\ = \frac{(1 - \rho_i^2)}{(1 + \rho_i^2 + 2\dot{\rho}_i')}\left(\frac{1}{Z_0}\right)V_i^2 \tag{57}$$

replacing a_i^2 from (54). Then be setting τ_i with (58) we get expression (59) for V_i:

$$\tau_i \equiv \sqrt{10^{-3}\, Z_0 \frac{(1 + \rho_i^2 + 2\dot{\rho}_i')}{(1 - \rho_i^2)}} \tag{58}$$

$$V_i = \tau_i\, 10^{\frac{\dot{P}_i'^{[dBm]}}{20}} \tag{59}$$

We suppose that we have available the (relative) magnitude frequency response for the magnitude of the input signal which in fact suggests linearity of the M function into the $\dot{V}_i$ variable:

$$K_i^{[dB]}(f) \equiv M_i^{[dBm]}(f, 0^{[dBm]}) - M_i^{[dBm]}(f_0, 0^{[dBm]}) \tag{60}$$

$$A_i^{[dB]}(f) \equiv K_i^{[dB]}(f) + M_i^{[dBm]}(f_0, 0^{[dBm]}) \tag{61}$$

$$M_i^{[dBm]}(f, \dot{P}_i'^{[dBm]}) = A_i^{[dB]}(f) + \dot{P}_i'^{[dBm]} \tag{62}$$

$$V_i = (\tau_i\, 10^{\frac{-A^{[dB]}(f)}{20}})\, 10^{\frac{\dot{M}_i^{[dBm]}(f, \dot{P}_i'^{[dBm]})}{20}} \tag{63}$$

Thus, we define a function

$$\boldsymbol{K}_i : \mathbf{f} \to \mathbf{A}_i;\ K_i = K_i(f) \equiv \\ \equiv \frac{M_i(f_i, V_{i_0})}{M_i(f_0, V_{i_0})} = \left(\frac{1}{M_{i_0}}\right)M_i(f_i, V_{i_0}) \tag{64}$$

where

$$M_{i_0} = M_i(f_0, V_{i_0}) \tag{65}$$

This suggests that linearity can be assumed to be hold in the second variable V_i:

$$\forall f \in \mathbf{f},\ \forall V_i \in \mathbf{V}_i,\ \exists ! M_i \in \mathbf{M}_i,$$

$$M_i = M_i(f, V_i) = M_i(f, V_i(\frac{V_{i_0}}{V_{i_0}})) =$$

$$= M_i(f, (\frac{V_i}{V_{i_0}})V_{i_0}) =$$

$$= (\frac{V_i}{V_{i_0}}) M_i(f, V_{i_0}) =$$

$$= (\frac{V_i}{V_{i_0}}) M_i(f, V_i = V_{i_0}) = \quad (66)$$

$$= (\frac{V_i}{V_{i_0}}) M_{i_0} K_i(f) = (\frac{M_{i_0}}{V_{i_0}}) K_i(f) V_i$$

In this way, we can define the function

$$\boldsymbol{A}_i : \mathbf{f} \to \mathbb{R} \quad (67)$$

$$\forall f \in \mathbf{f},\ \exists ! k \in \mathbb{R},$$

$$k = A_i(f) \equiv (\frac{M_{i_0}}{V_{i_0}}) K_i(f) \quad (68)$$

so that finally

$$\forall f \in \mathbf{f},\ \forall V_i \in \mathbf{V}_i,\ \exists ! M_i \in \mathbf{M}_i,$$

$$M_i = M_i(f, V_i) = A_i(f) V_i \quad (69)$$

A5b. Input signals ratio measurements

Initially we define the ratio of the input signals from the

$$\dot{\boldsymbol{v}} : \dot{\mathbf{V}}_A \times \dot{\mathbf{V}}_R \to \dot{\mathbb{C}} \quad (70)$$

$$\forall \dot{V}_A \in \dot{\mathbf{V}}_A,\ \forall \dot{V}_R \in \dot{\mathbf{V}}_R,$$

$$\dot{v} = \dot{v}(\dot{V}_A, \dot{V}_R) \equiv \frac{\dot{V}_A}{\dot{V}_R} \text{ with } \dot{V}_R \neq \dot{0} \quad (71)$$

so that the set of resulting values is the image

$$\dot{\mathbf{v}} \equiv \dot{\boldsymbol{v}} [\, \dot{\mathbf{V}}_A \times \dot{\mathbf{V}}_R \,] \quad (72)$$

After this we have for the magnitude of the ratio:

$$\mathbf{v} \equiv [\, v_m, v_M \,] = \{ v \equiv |\dot{v}| \,|\, (0 < v_m \equiv$$

$$\equiv \frac{V_{i_m}}{V_{i_M}} \leq v \leq v_M \equiv \frac{V_{i_M}}{V_{i_m}}) \} \subset \mathbb{R}_+ \quad (73)$$

Let

$$\hat{V} \equiv \hat{V}_A - \hat{V}_R \quad (74)$$

then the phase of $\dot{v}$ is

$$\hat{v} \equiv \measuredangle(\frac{\dot{V}_A}{\dot{V}_R}) \quad (75)$$

which belongs to the set $\hat{\mathbf{v}}$ defined by the following property:

$$\hat{V} \in \begin{Bmatrix} (-2\pi, -\pi] \\ (\pi, +\pi] \\ (\pi, 2\pi] \end{Bmatrix} \Rightarrow \hat{v} = \hat{V} + \begin{cases} 2\pi \\ 0 \\ -2\pi \end{cases} \quad (76)$$

The ratio measurements can be described now by the functions:

$$\boldsymbol{m} : \mathbf{f} \times \mathbf{v} \to \mathbf{m} \quad (77)$$

and

$$\hat{\boldsymbol{m}} : \mathbf{f} \times \hat{\mathbf{v}} \to \hat{\mathbb{m}} \tag{78}$$

so the measurements can be represented by the function

$$\dot{\boldsymbol{m}} : \mathbf{f} \times \dot{\mathbf{v}} \to \dot{\mathbb{m}};\ \forall \mathrm{f} \in \mathbf{f},\ \forall \dot{\mathrm{v}} \in \dot{\mathbf{v}},$$

$$\dot{m}(\mathrm{f}, \dot{\mathrm{v}}) \equiv m(\mathrm{f}, \mathrm{v}) e^{i\hat{m}(\mathrm{f}, \hat{\mathrm{v}})} \tag{79}$$

It is supposed now, that we have available a magnitude and a phase relative frequency responses from the two different input channels (fa, fb), which, as above, can be described by the functions:

$$\boldsymbol{k} : \mathbf{f} \to \mathbb{R};\ \forall \mathrm{f} \in \mathbf{f},\ \exists!\, \mathrm{k} \in \mathbb{R},$$

$$\mathrm{k} = k(\mathrm{f}) \equiv \frac{m(\mathrm{f}, \mathrm{v}_0)}{m(\mathrm{f}_a, \mathrm{v}_0)} \tag{80}$$

$$\hat{\boldsymbol{k}} : \mathbf{f} \to \mathbb{R};\ \forall \mathrm{f} \in \mathbf{f},\ \exists!\, \hat{\mathrm{k}} \in \mathbb{R}, \tag{81}$$

$$\hat{\mathrm{k}} = \hat{k}(\mathrm{f}) \equiv \hat{m}(\mathrm{f}, \hat{\mathrm{v}}_0) - \hat{m}(\mathrm{f}_b, \hat{\mathrm{v}}_0) + \nu(2\pi)$$

where

$$\nu \in \{-1, 0, 1\} \tag{82}$$

as above, in order to keep $\hat{\mathrm{k}}$ into $(-\pi, \pi]$.

$$\dot{\boldsymbol{k}} : \mathbf{f} \to \dot{\mathbb{C}};\ \forall \mathrm{f} \in \mathbf{f},\ \exists!\, \dot{\mathrm{k}} \in \dot{\mathbb{C}},$$

$$\dot{\mathrm{k}} = \dot{k}(\mathrm{f}) \equiv k(\mathrm{f}) e^{i\hat{\mathrm{k}}(\mathrm{f})} =$$

$$= \frac{m(\mathrm{f}, \mathrm{v}_0)}{m(\mathrm{f}_a, \mathrm{v}_0)} e^{i(\hat{m}(\mathrm{f}, \hat{\mathrm{v}}_0) - \hat{m}(\mathrm{f}_b, \hat{\mathrm{v}}_0))} e^{i\nu(2\pi)} =$$

$$= \frac{m(\mathrm{f}, \mathrm{v}_0) e^{i\hat{m}(\mathrm{f}, \hat{\mathrm{v}}_0)}}{m(\mathrm{f}_a, \mathrm{v}_0) e^{i\hat{m}(\mathrm{f}_b, \hat{\mathrm{v}}_0)}} \tag{83}$$

Usually

$$\mathrm{f}_a = \mathrm{f}_0 = \mathrm{f}_b \tag{84}$$

so that

$$m(\mathrm{f}_a, \mathrm{v}_0) e^{i\hat{m}(\mathrm{f}_b, \hat{\mathrm{v}}_0)} =$$

$$= m(\mathrm{f}_0, \mathrm{v}_0) e^{i\hat{m}(\mathrm{f}_0, \hat{\mathrm{v}}_0)} \equiv$$

$$\equiv \dot{m}(\mathrm{f}_0, \dot{\mathrm{v}}_0) \equiv \dot{\mathbb{m}}_0 \tag{85}$$

and finally

$$\dot{k}(\mathrm{f}) \equiv \left(\frac{1}{\dot{\mathbb{m}}_0}\right) \dot{m}(\mathrm{f}, \dot{\mathrm{v}}_0) \tag{86}$$

As before, we also assume linearity in the second complex variable and in this way, for the complex frequency response [8]

$$\forall \mathrm{f} \in \mathbf{f},\ \forall \dot{\mathrm{v}} \in \dot{\mathbf{v}},\ \exists!\, \dot{\mathbb{m}} \in \dot{\mathbb{m}},$$

$$\dot{\mathbb{m}} = \dot{m}(\mathrm{f}, \dot{\mathrm{v}}) = \dot{m}\left(\mathrm{f}, \dot{\mathrm{v}}\left(\frac{\dot{\mathrm{v}}_0}{\dot{\mathrm{v}}_0}\right)\right) = \ldots$$

$$= \left(\frac{\dot{\mathbb{m}}_0}{\dot{\mathrm{v}}_0}\right) \dot{k}(\mathrm{f}) \dot{\mathrm{v}} \tag{87}$$

$$\dot{\boldsymbol{\alpha}} : \mathbf{f} \to \dot{\mathbb{C}};\ \forall \mathrm{f} \in \mathbf{f},\ \exists!\, \dot{\alpha} \in \dot{\mathbb{C}},$$

$$\dot{\alpha} = \dot{\alpha}(\mathrm{f}) \equiv \left(\frac{\dot{\mathbb{m}}_0}{\dot{\mathrm{v}}_0}\right) \dot{k}(\mathrm{f}) \tag{88}$$

$$\boxed{\dot{\mathbb{m}} = \dot{m}(\mathrm{f}, \dot{\mathrm{v}}) = \dot{\alpha}(\mathrm{f}) \dot{\mathrm{v}}} \tag{89}$$

B. The DUT

If Z_0 is the common real value of the characteristic impedance for the totality of the involved devices and we intend to measure only passive DUTs then the set of all possible reflection coefficients values $\dot{\rho}$ [9] is

$$\dot{\boldsymbol{\rho}} \equiv \{\dot{\rho} \mid 0 \le |\dot{\rho}| \le 1 \subset \dot{\mathbb{C}} \qquad (90)$$

$$\dot{\boldsymbol{\rho}}_t : \mathbf{f} \to \dot{\boldsymbol{\rho}};\ \dot{\rho}_t \equiv \rho_t(f)$$

Geometrically, the sets $\dot{\mathbf{V}}_G$, $\dot{\mathbf{V}}_A$, $\dot{\mathbf{V}}_R$ and $\dot{\mathbf{m}}$ are annuluses around the origin O of the $\dot{\mathbb{C}}$ plane, the set $\dot{\boldsymbol{\rho}}$ is the unit circle with center at O and the sets $\mathbf{M_A}$ and $\mathbf{M_R}$ are segments of the positive real axis $\mathbb{R}_+$.The shape of the defined sets is shown in Fig. 4.

C. The IE

C1. The operation

We attempt to describe the IE operation by considering (Fig. 2) that the stimulus signal $\dot{v}_g$ at the IE input port G in the presence of the DUT's $\dot{\rho}$ at IE port T, causes a pair of signals $\dot{v}_a$ and $\dot{v}_r$ to arise at the IE output ports A and R respectively. Obviously

$$\dot{\boldsymbol{v}}_g \subseteq \dot{\mathbf{V}}_0 \qquad (91)$$

and furthermore we accept that the IE operation is described by a pair of smooth functions

$$\dot{\boldsymbol{v}}_a : \dot{\boldsymbol{\rho}} \times \dot{\mathbf{v}}_g \to \dot{\mathbf{V}}_A \qquad (92)$$

$$\dot{\boldsymbol{v}}_r : \dot{\boldsymbol{\rho}} \times \dot{\mathbf{v}}_g \to \dot{\mathbf{V}}_R \qquad \{93)$$

and to avoid unnecessary complications between the produced and allowable voltage levels, we can accept that

$$\dot{\boldsymbol{v}}_a [\dot{\boldsymbol{\rho}} \times \dot{\mathbf{v}}_G] = \dot{\mathbf{v}}_a \subseteq \dot{\mathbf{V}}_A \text{ and} \qquad (94)$$

$$\dot{\boldsymbol{v}}_r [\dot{\boldsymbol{\rho}} \times \dot{\mathbf{v}}_G] = \dot{\mathbf{v}}_r \subseteq \dot{\mathbf{V}}_R \qquad (95)$$

In this way we have for the VNA signals

$$\dot{V}_G = \dot{v}_G,\ \dot{V}_A = \dot{v}_a,\ \dot{V}_R = \dot{v}_r,$$

$$\dot{v} = \frac{\dot{V}_A}{\dot{V}_R} = \frac{\dot{v}_a}{\dot{v}_r} \qquad (96)$$

The IE can be viewed as a four port junction represented by the flow graph of Fig. 5 and described by the S-parameter matrix:

$$[\dot{S}] = \begin{bmatrix} \dot{S}_{GG} & \dot{S}_{GA} & \dot{S}_{GR} & \dot{S}_{GT} \\ \cdots & \cdots & \cdots & \cdots \\ \dot{S}_{AG} & \dot{S}_{AA} & \dot{S}_{AR} & \dot{S}_{AT} \\ \cdots & \cdots & \cdots & \cdots \\ \dot{S}_{RG} & \dot{S}_{RA} & \dot{S}_{RR} & \dot{S}_{RT} \\ \cdots & \cdots & \cdots & \cdots \\ \dot{S}_{TG} & \dot{S}_{TA} & \dot{S}_{TR} & \dot{S}_{TT} \end{bmatrix} \qquad (97)$$

If we shall use the wave-voltage signal equations in the only one propagated TEM

mode at the frequency f then: If

$$\dot{\alpha}_x, \dot{\beta}_x \text{ and } \dot{a}_x, \dot{b}_x \qquad (98)$$

are the levels of the incoming and outgoing voltage waves at port

$$x = g, a, r, t, G, A, R, T \qquad (99)$$

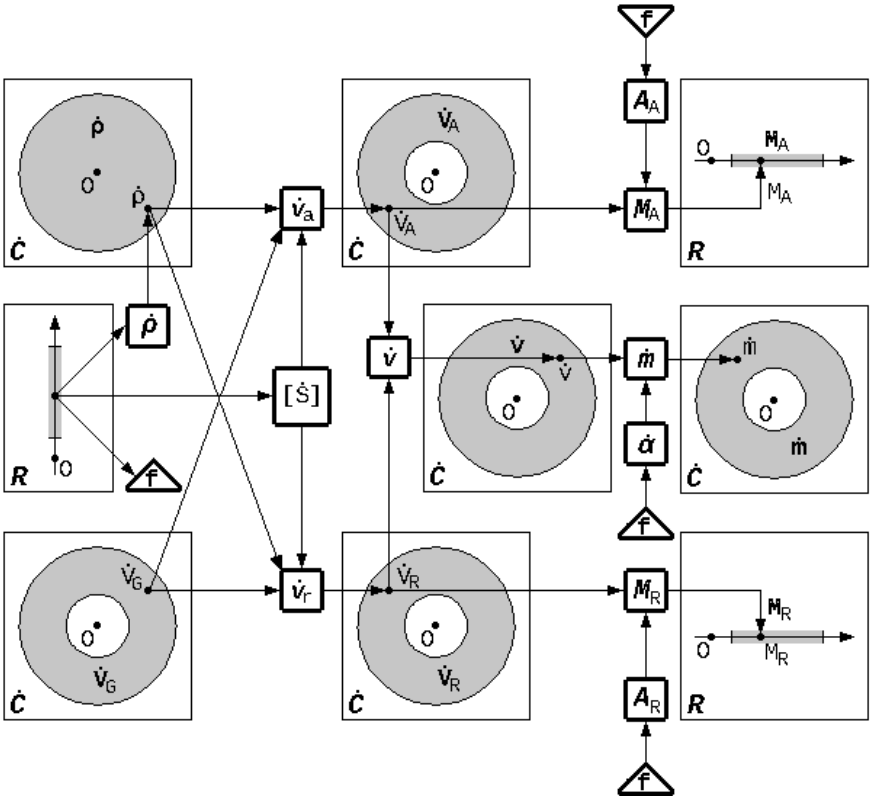

Fig. 4: The sets $\dot{\mathbf{V}}_G, \mathbf{f}, \dot{\boldsymbol{\rho}}, \dot{\mathbf{V}}_A, \dot{\mathbf{V}}_R, \dot{\mathbf{v}}, \dot{\mathbf{m}}, \mathbf{M_A}, \mathbf{M_R}$

of the VNA and IE respectively, as in (3) above, we have in vector-one column matrix notation:

$$[\dot{\alpha}] \equiv \bar{\alpha} = \bar{b} \equiv [\dot{b}] \qquad (100a)$$

$$[\dot{\beta}] \equiv \bar{\beta} = \bar{a} \equiv [\dot{a}] \qquad (100b)$$

$$\dot{V}_x = (\dot{\beta}_x + \dot{\alpha}_x)\sqrt{Z_0} = (\dot{a}_x + \dot{b}_x)\sqrt{Z_0} \qquad (101)$$

$$[\dot{\beta}] = [\dot{S}][\dot{\alpha}] \qquad (102)$$

$$[\dot{a}] = [\dot{S}][\dot{b}] \qquad (103)$$

but at each one of the ports we have the conditions

$$\dot{b}_G = \dot{\rho}_G \dot{a}_G + \dot{e}_G \tag{104a}$$

$$\dot{b}_A = \dot{\rho}_A \dot{a}_A \tag{104b}$$

$$\dot{b}_R = \dot{\rho}_R \dot{a}_R \tag{104c}$$

$$\dot{b}_T = \dot{\rho}_T \dot{a}_T \tag{104d}$$

or in matrix form

$$[\dot{b}] = [\dot{\rho}]^t [I][\dot{a}] + [\dot{e}] \tag{105}$$

and if $[\dot{S}]^{-1} \neq 0$ then (106)

$$[\dot{S}]^{-1}[\dot{a}] = [\dot{\rho}]^t [I][\dot{a}] + [\dot{e}] \tag{107}$$

$$([\dot{S}]^{-1} - [\dot{\rho}]^t [I])[\dot{a}] = [\dot{e}] \tag{108}$$

$$[\dot{\tilde{S}}] \equiv ([\dot{S}]^{-1} - [\dot{\rho}]^t [I]) \tag{109}$$

$$\dot{v} = \frac{\dot{V}_A}{\dot{V}_R} = \frac{\sqrt{Z_0}(\dot{a}_A + \dot{b}_A)}{\sqrt{Z_0}(\dot{a}_R + \dot{b}_R)} =$$

$$= \left(\frac{1 + \dot{\rho}_A}{1 + \dot{\rho}_R}\right)\left(\frac{\dot{a}_A}{\dot{a}_R}\right) = \dot{\sigma}\left(\frac{\dot{a}_A}{\dot{a}_R}\right) \tag{110}$$

$$\dot{\sigma} \equiv \left(\frac{1 + \dot{\rho}_A}{1 + \dot{\rho}_R}\right) \tag{111}$$

$$\frac{\dot{a}_A}{\dot{a}_R} = -\frac{|[\dot{\tilde{S}}_{GA}]|}{|[\dot{\tilde{S}}_{GR}]|} = \frac{-|[\dot{\tilde{S}}_{GA}]_{TG}|\,\dot{\tilde{S}}_{TG} + |[\dot{\tilde{S}}_{GA}]_{TR}|\,\dot{\tilde{S}}_{TR} - |[\dot{\tilde{S}}_{GA}]_{TT}|\,\dot{\tilde{S}}_{TT}}{|[\dot{\tilde{S}}_{GR}]_{TG}|\,\dot{\tilde{S}}_{TG} - |[\dot{\tilde{S}}_{GR}]_{TA}|\,\dot{\tilde{S}}_{TA} + |[\dot{\tilde{S}}_{GR}]_{TT}|\,\dot{\tilde{S}}_{TT}} =$$

$$= \frac{(-|[\dot{\tilde{S}}_{GA}]_{TG}|\,\dot{\tilde{S}}_{TG} + |[\dot{\tilde{S}}_{GA}]_{TR}|\,\dot{\tilde{S}}_{TR} - |[\dot{\tilde{S}}_{GA}]_{TT}|\,\dot{S}_{TT}^{-1}) + |[\dot{\tilde{S}}_{GA}]_{TT}|\,\dot{\rho}_T}{(|[\dot{\tilde{S}}_{GR}]_{TG}|\,\dot{\tilde{S}}_{TG} - |[\dot{\tilde{S}}_{GR}]_{TA}|\,\dot{\tilde{S}}_{TA} + |[\dot{\tilde{S}}_{GR}]_{TT}|\,\dot{S}_{TT}^{-1}) - |[\dot{\tilde{S}}_{GR}]_{TT}|\,\dot{\rho}_T} \tag{112}$$

Setting

$$\dot{A} \equiv |[\dot{\tilde{S}}_{GA}]_{TT}| \tag{113}$$

$$\dot{B} \equiv (-|[\dot{\tilde{S}}_{GA}]_{TG}|\,\dot{\tilde{S}}_{TG} + |[\dot{\tilde{S}}_{GA}]_{TR}|\,\dot{\tilde{S}}_{TR} - |[\dot{\tilde{S}}_{GA}]_{TT}|\,\dot{S}_{TT}^{-1}) \tag{114}$$

$$\dot{\Gamma} \equiv -|[\dot{\tilde{S}}_{GR}]_{TT}| \tag{115}$$

$$\dot{\Delta} \equiv (|[\dot{\tilde{S}}_{GR}]_{TG}|\,\dot{\tilde{S}}_{TG} - |[\dot{\tilde{S}}_{GR}]_{TA}|\,\dot{\tilde{S}}_{TA} + |[\dot{\tilde{S}}_{GR}]_{TT}|\,\dot{S}_{TT}^{-1}) \tag{116}$$

then from (110) and (111)

$$\dot{v} = \dot{\sigma}\left(\frac{\dot{A}\dot{\rho} + \dot{B}}{\dot{\Gamma}\dot{\rho} + \dot{\Delta}}\right) = \frac{(\dot{\sigma}\dot{A})\dot{\rho} + (\dot{\sigma}\dot{B})}{(\dot{\Gamma})\dot{\rho} + (\dot{\Delta})} \tag{117}$$

and from (89) the measurement $\dot{m}$ is given by

$$\dot{m} = \dot{m}(f, \dot{v}) = \dot{\alpha}(f)\dot{v} = \dot{\alpha}(f)\dot{\sigma}\left(\frac{\dot{a}_A}{\dot{a}_R}\right) =$$

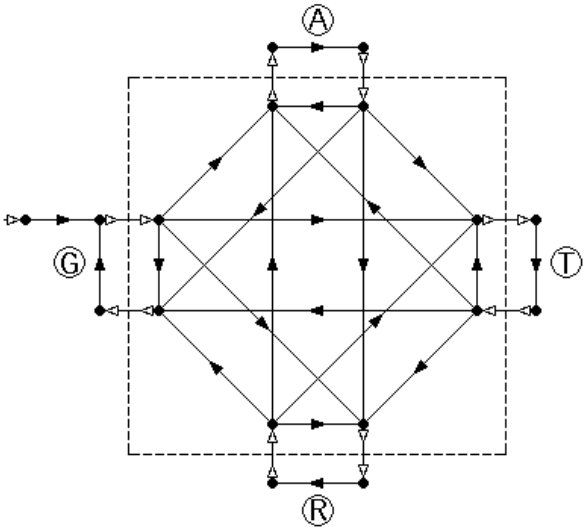

Fig. 5: The four port junction flow graph of the IE

$$= \dot{\alpha}(f)\dot{\sigma}\left(\frac{\dot{A}\dot{\rho} + \dot{B}}{\dot{\Gamma}\dot{\rho} + \dot{\Delta}}\right) \qquad (118)$$

Error Parameters Formulation

It is given [1] that in network analyzer measurements with one port error model are involved initially five complex quantities, named as

$\dot{\rho}$ for the reflection coefficient of the unknown load,

$\dot{m}$ for its measured value,

$\dot{D}$ for the directivity error,

$\dot{M}$ for the source match error and

$\dot{R}$ for the frequency response error which equals to $(1+\dot{T})$, where $\dot{T}$ stands for the reflection tracking error.

The above quantities are shown in the well known flow graph of Fig. 6 [10], [11] and verify the relation

$$\dot{m} = \dot{D} + \frac{\dot{R}\dot{\rho}}{1 - \dot{M}\dot{\rho}} \qquad (119)$$

which is the starting point of our discussion and with a re-arrangement becomes

$$\dot{m} = \frac{(\dot{R} - \dot{D}\dot{M})\dot{\rho} + (\dot{D})}{(-\dot{M})\dot{\rho} + (1)} \qquad (120)$$

and from (118)

$$\dot{m} = \frac{(\frac{\dot{\alpha}(f)\dot{\sigma}\dot{A}}{\dot{\Delta}})\dot{\rho} + (\frac{\dot{\alpha}(f)\dot{\sigma}\dot{B}}{\dot{\Delta}})}{(\frac{\dot{\Gamma}}{\dot{\Delta}})\dot{\rho} + (1)} \quad (121)$$

where

$$\dot{M} \equiv -(\frac{\dot{\Gamma}}{\dot{\Delta}}) \quad (122a)$$

$$\dot{D} \equiv (\frac{\dot{\alpha}(f)\dot{\sigma}\dot{B}}{\dot{\Delta}}) \quad (122b)$$

$$\dot{R} \equiv (\frac{\dot{\alpha}(f)\dot{\sigma}\dot{A}}{\dot{\Delta}}) - (\frac{\dot{\Gamma}}{\dot{\Delta}})(\frac{\dot{\alpha}(f)\dot{\sigma}\dot{B}}{\dot{\Delta}}) \quad (122c)$$

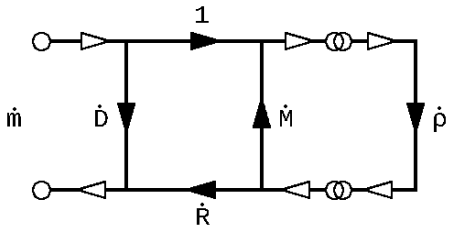

Fig. 6: One port error model

We are interested of course to compute $\dot{\rho}$, hence by (119), we have

$$\dot{\rho} = \frac{\dot{m} - \dot{D}}{\dot{M}(\dot{m} - \dot{D}) + \dot{R}} \quad (123a)$$

and in as a typically bilinear function form [2]

$$\dot{\rho} = \frac{(1)\dot{m} + (-\dot{D})}{(\dot{M})\dot{m} + (\dot{R} - \dot{M}\dot{D})} \quad (123b)$$

which is characterized by the constants 1, $-\dot{D}$, $\dot{M}$, $\dot{R} - \dot{M}\dot{D}$ or by defining

$$\dot{Q} \equiv \dot{R} - \dot{M}\dot{D} \quad (124)$$

we take finally

$$\dot{\rho} = \frac{\dot{m} - \dot{D}}{\dot{M}\dot{m} + \dot{Q}} \quad (125)$$

By re-arranging the terms of (125) we take in array-vector form

$$\begin{bmatrix} \dot{\rho} & \vdots & \dot{\rho}\dot{m} & \vdots & 1 \end{bmatrix} \begin{bmatrix} \dot{Q} \\ \cdots \\ \dot{M} \\ \cdots \\ \dot{D} \end{bmatrix} = \dot{m} \quad (126)$$

We find the constants of the bilinear transformation by applying the "One Port Full Calibration Method" [1] and defining Standard Loads $\dot{S}$, $\dot{L}$, $\dot{O}$, and their respective measurements $\dot{s}$, $\dot{l}$, $\dot{o}$, as follows

$\dot{S},\dot{s}$: for "Shortcircuit" with typical value –1,

$\dot{L}$, $\dot{l}$: for "matching Load", tyically 0 and

$\dot{O}$, $\dot{o}$: for "Opencircuit", typically 1.

We have from (126) in matrix form

$$\begin{bmatrix} \dot{O} & \vdots & \dot{O}\dot{o} & \vdots & 1 \\ \cdots & \vdots & \cdots & \vdots & \cdots \\ \dot{S} & \vdots & \dot{S}\dot{s} & \vdots & 1 \\ \cdots & \vdots & \cdots & \vdots & \cdots \\ \dot{L} & \vdots & \dot{L}\dot{l} & \vdots & 1 \end{bmatrix} \begin{bmatrix} \dot{Q} \\ \cdots \\ \dot{M} \\ \cdots \\ \dot{D} \end{bmatrix} = \begin{bmatrix} \dot{o} & \vdots & \dot{s} & \vdots & \dot{l} \end{bmatrix} \quad (127)$$

We define as

$$\dot{A} \equiv \begin{bmatrix} \dot{O} & \dot{O}\dot{o} & 1 \\ \cdots & \cdots & \cdots \\ \dot{S} & \dot{S}\dot{s} & 1 \\ \cdots & \cdots & \cdots \\ \dot{L} & \dot{L}\dot{l} & 1 \end{bmatrix} \tag{128}$$

The determinant of $\dot{A}$ is

$$[\dot{A}] = \dot{O}(\dot{L} - \dot{S})\dot{o} + \dot{S}(\dot{O} - \dot{L})\dot{s} + \\ + \dot{L}(\dot{S} - \dot{O})\dot{l} \tag{129}$$

At this point we note that the manipulation of the rather lengthy expressions is greatly facilitated by the observation of the cyclic nature of the forms over the letters S,L,O and s,l,o respectively. By the introduction of the symbol $\sum_{\circ}$ for the cyclic summation we have [11]

$$\boxed{[\dot{A}] = \sum_{\circ} \dot{o}\dot{O}(\dot{L} - \dot{S})} \tag{130}$$

The inverse of $\dot{A}$ is

$$\dot{A}^{-1} = \begin{bmatrix} \dot{O} & \dot{O}\dot{o} & 1 \\ \cdots & \cdots & \cdots \\ \dot{S} & \dot{S}\dot{s} & 1 \\ \cdots & \cdots & \cdots \\ \dot{L} & \dot{L}\dot{l} & 1 \end{bmatrix}^{-1} = \frac{1}{[\dot{A}]} \begin{bmatrix} \dot{S}\dot{s} - \dot{L}\dot{l} & \dot{L}\dot{l} - \dot{O}\dot{o} & \dot{O}\dot{o} - \dot{S}\dot{s} \\ \cdots & \cdots & \cdots \\ \dot{L} - \dot{S} & \dot{O} - \dot{L} & \dot{S} - \dot{O} \\ \cdots & \cdots & \cdots \\ \dot{S}\dot{L}(\dot{l} - \dot{s}) & \dot{O}\dot{L}(\dot{o} - \dot{l}) & \dot{O}\dot{S}(\dot{s} - \dot{o}) \end{bmatrix} \tag{131}$$

and the solution of the system is

$$\begin{bmatrix} \dot{Q} \\ \cdots \\ \dot{M} \\ \cdots \\ \dot{D} \end{bmatrix} = \frac{1}{[\dot{A}]} \begin{bmatrix} \dot{S}\dot{s} - \dot{L}\dot{l} & \dot{L}\dot{l} - \dot{O}\dot{o} & \dot{O}\dot{o} - \dot{S}\dot{s} \\ \cdots & \cdots & \cdots \\ \dot{L} - \dot{S} & \dot{O} - \dot{L} & \dot{S} - \dot{O} \\ \cdots & \cdots & \cdots \\ \dot{S}\dot{L}(\dot{l} - \dot{s}) & \dot{O}\dot{L}(\dot{o} - \dot{l}) & \dot{O}\dot{S}(\dot{s} - \dot{o}) \end{bmatrix} \begin{bmatrix} \dot{o} \\ \cdots \\ \dot{s} \\ \cdots \\ \dot{l} \end{bmatrix} \tag{132}$$

or in the cyclic form

$$\dot{Q} = \frac{1}{[\dot{A}]} \sum_{\circ} \dot{s}\dot{l}(\dot{L} - \dot{S}) \tag{133}$$

$$\dot{M} = \frac{1}{[\dot{A}]} \sum_{\circ} \dot{o}(\dot{L} - \dot{S}) \tag{134}$$

$$\dot{D} = -\frac{1}{[\dot{A}]} \sum_{\circ} \dot{s}\dot{l}\dot{O}(\dot{L} - \dot{S}) \tag{135}$$

$$\dot{R} = \frac{1}{[\dot{A}]} \prod_{\circ} (\dot{S} - \dot{L})(\dot{s} - \dot{l}) \tag{136}$$

and thus (125) becomes [12]

$$\dot{\rho} = \frac{\dot{S}(\dot{L} - \dot{O})(\dot{m}\dot{s} + \dot{l}\dot{o}) + \dot{L}(\dot{O} - \dot{S})(\dot{m}\dot{l} + \dot{o}\dot{s}) + \dot{O}(\dot{S} - \dot{L})(\dot{m}\dot{o} + \dot{s}\dot{l})}{(\dot{L} - \dot{O})(\dot{m}\dot{s} + \dot{l}\dot{o}) + \ (\dot{O} - \dot{S})(\dot{m}\dot{l} + \dot{o}\dot{s}) + \ (\dot{S} - \dot{L})(\dot{m}\dot{o} + \dot{s}\dot{l})} \tag{137}$$

In the measurement system in use, the "other support devices" of Fig. 2 included mainly a Phase Locked arrangement with 100Hz step signal generator, a 10-digits frequency counter ([13] - [15]) and a personal computer which runs developed by us (therefore completely manageable) software in IEEE-488 for the device control, in Visual Basic for the data collection and in Mathematica for the data processing ([16] – [22]).

Practical Applications

The VNA characteristics as sets of values are given in [23] - [25]. Tab. 1 gives only those characteristics that are clearly stated and related exclusively to reflection measurements. Tab. 2 contains some of the performance tests that were performed and again are related only to the reflection measurements [26]. The HP909A male standard load was used as matching load.

To construct the $\dot{v}$ function, with its value $\dot{v}$ to be given through (110) we start from a given circuit diagram for the T/R Test Set [26]. In Fig. 7 we have simplified this circuit along with the IE's transmission lines (TLs).

In the equivalent circuit which is actually an RF simplification of the original, we have omitted:

(i) The bias circuitry (input connector, feed-through capacitor, RF chock and all the other blocking capacitors), and

(ii) The step attenuator and its corresponding electrical length compensation transmission line segments, because we do not use them. On the other hand we have assumed properly formed values for the resistors of the pad. In the circuit of Fig. 7 are readily recognized.

It is obvious that the rest of the elements can be thought as they form a power divider - directional bridge combination supported by the compensation pad and by the isolation transformer with a detail note that the pad’s resistor values are taken by implication based on the rest of the circuit characteristics. Our study is limited by the extent of our knowledge about the characteristics of the various devices involved. In order to clear once at all the role-played by the T/R Test Set in forming the relation between $\dot{m}, \dot{Z}$ we analyze its equivalent circuit as it is shown in Fig. 8.

Tab. 1: VNA characteristics for reflection measurements

$\widetilde{\mathbf{P}}_0$ [dBm]	–72 - +10
Input Level [dBm]	–10 or –30
f [MHz]	0.5 - 1300
Dynamic Range $\widetilde{\mathbf{M}}_i$[dBm]	–110 - –10
Dynamic Range **v** [dB]	100
$\mathbf{M}_i$ [dB]	–199.99 - +199.99
Magnitude HPIB [dB]	xxx.xx
Phase [°]	–180 - +180
Phase HPIB [°]	xxxx.x

Tab. 2: Performance test record for reflection measurements

Description	Lower Limit	Measured Value	Upper Limit
Directivity [dB]	40	43.3	
Transmission Frequency Response			
MAG [dB]:		0.7	0.8
PHASE [°]:		5	8
Reflection Frequency Response			
MAG [dB]: 0.5 - 1300 MHz		0.4	1.5
PHASE [°]: 0.5 - 1300 MHz		2.5	15
PHASE [°]: 2 - 1300 MHz		2	10
Test Port Open/Short Ratio			
MAG [dB]: 1000 - 1300 MHz		0.54	1.8
PHASE [°]: 1000 - 1300 MHz		8	15
MAG [dB]: 2 - 1300 MHz		0.3	1.5
PHASE [°]: 2 - 1300 MHz		6.5	12
MAG [dB]: 0.5 - 2 MHz		1.9	2.5
PHASE [°]: 0.5 - 2 MHz		5.6	20

Description	Lower	Measured	Upper
Magnitude Reference Offset and Marker Accuracy Test			
Rectangular marker Zero [dB]	–0.01	0.00	+0.01
Polar Marker Zero - Magnitude of Outside circle	–3 mm	0	+3 mm
Polar marker Zero - Phase [°]	–1	0	+1
Offset +190 dB & read marker	–184	–190.1	–196
Offset –190 dB & read marker	+184	+190	+196
Crosstalk Isolation [dB]			
Crosstalk between R and A Port	100	–117.3	
Crosstalk between A and R Port	100	–119.2	
Magnitude and Phase Frequency Response			
Port R [dB]		2	3
Port A [dB]		2	3
A/R Ratio Magnitude [dB]		0.47	0.6
A/R Ratio Phase [°]:			
0.5 - 750 MHz		6	6
750 – 1300 MHz		4	10
Phase Reference Offset			
Reference Offset, CRT trace tolerance from reference line:			
±360°	–2.1	0.8	+2.1
±720°	–3.9	1.5	+3.9
±1080°	–5.7	2.0	+5.7
±1440°	–7.0	2.6	+7.5
Phase Accuracy Test			
+180° transition	+182	181	+178
–180° transition	–182	–180	–178
Input Impedance Test			
Return Loss of Port A [dB]	20	–25	
Return Loss of Port R [dB]	20	–23	
Source Impedance Test			
SWR of RF OUTPUT port		1.15	1.38

Indices for ports are as page oriented: L-R-U-D (Left, Right, Up, Down). The S-parameter matrix

$$[\dot{S}^X] = \begin{bmatrix} \dot{S}^X_{ii} & \vdots & \dot{S}^X_{ij} \\ \cdots & \vdots & \cdots \\ \dot{S}^X_{ji} & \vdots & \dot{S}^X_{jj} \end{bmatrix} =$$

$$= \begin{bmatrix} 0 & \vdots & e^{-\dot{\gamma}^X L^X} \\ \cdots & \vdots & \cdots \\ e^{-\dot{\gamma}^X L^X} & \vdots & 0 \end{bmatrix} \qquad (138)$$

stands for the IE's transmission lines, where

X = H, I, J, K

$\dot{\gamma}$ is the well known propagation factor $\alpha + i\beta$

L is the length of the line.

The transformer F can be described by the matrix

$$[\dot{S}^F] = \begin{bmatrix} \dot{S}^F_{ll} & \vdots & \dot{S}^F_{lr} \\ \cdots & \vdots & \cdots \\ \dot{S}^F_{rl} & \vdots & \dot{S}^F_{rr} \end{bmatrix} = \begin{bmatrix} 0 & \vdots & 1 \\ \cdots & \vdots & \cdots \\ 1 & \vdots & 0 \end{bmatrix} \qquad (139)$$

The compensation pad C

$$[\dot{S}^C] = \begin{bmatrix} \dot{S}^C_{dd} & \vdots & \dot{S}^C_{du} \\ \cdots & \vdots & \cdots \\ \dot{S}^C_{ud} & \vdots & \dot{S}^F_{uu} \end{bmatrix} = \begin{bmatrix} 0 & \vdots & \frac{1}{4} \\ \cdots & \vdots & \cdots \\ \frac{1}{4} & \vdots & 0 \end{bmatrix} \qquad (140)$$

The power divider P by matrix (141) and the directional bridge B by matrix (142).

Now that we know the S-parameters of all the components parts of the T/R Set circuit (Fig. 7) we can use the flow graph techniques-rules [27], [28] and the topology of the graph of Fig. 8 to determine the S-parameters of the equivalent four port (Fig. 5) and by means of them to express $\dot{v}$ and finally $\dot{m}$. Thus we obtain the matrix (143) for the $[\dot{S}]$ matrix of (97).

In the most simplified case where the transmission lines H, I, J and K are substituted by ideal connectors which implies that the secondary diagonal elements of $[\dot{S}^X]$ matrices are unitary, the $[\dot{S}]$ matrix becomes real (144).

In order to illustrate the above result we redraw Fig. 5 and obtain Fig. 9. From (144), (110) and Fig. 9, and since $\dot{\sigma} = 1$ for matched ports A, R with $\dot{\rho}_A = 0 = \dot{\rho}_R$, we have for $\dot{v}$

$$\frac{\dot{a}_A}{\dot{a}_R} = \frac{\dot{S}_{AG} + (\dot{S}_{AT}\dot{S}_{TG} - \dot{S}_{TT}\dot{S}_{AG})\dot{\rho}}{\dot{S}_{RG} + (\dot{S}_{RT}\dot{S}_{TG} - \dot{S}_{TT}\dot{S}_{RG})\dot{\rho}} =$$

$$= \frac{0 + (\frac{1}{2}\times\frac{1}{4} - \frac{1}{16}0)\dot{\rho}}{\frac{1}{8} + (\frac{1}{32}\times\frac{1}{4} - \frac{1}{16}\times\frac{1}{8})\dot{\rho}} =$$

$$= \frac{\frac{1}{8}\dot{\rho}}{\frac{1}{8}} = \dot{\rho} \qquad (145)$$

as we expected for this ideal case.

If we return to the most general case which indicates the existence of the H, I, J, K different transmission lines then the $[\dot{S}]$ matrix and the above ratio of the incoming voltage waves at A and R ports of the VNA we take the expressions (146) and (147) respectively.

$$[\dot{S}^P] = \begin{bmatrix} \dot{S}^P_{ll} & \vdots & \dot{S}^P_{lu} & \vdots & \dot{S}^P_{lr} \\ \cdots & \vdots & \cdots & \vdots & \cdots \\ \dot{S}^P_{ul} & \vdots & \dot{S}^P_{uu} & \vdots & \dot{S}^P_{ur} \\ \cdots & \vdots & \cdots & \vdots & \cdots \\ \dot{S}^P_{rl} & \vdots & \dot{S}^P_{ru} & \vdots & \dot{S}^P_{rr} \end{bmatrix} = \frac{1}{3+\dot{\zeta}} \begin{bmatrix} \dot{\zeta}-1 & \vdots & 2 & \vdots & 2 \\ \cdots & \vdots & \cdots & \vdots & \cdots \\ 2 & \vdots & \dfrac{(1+\dot{\zeta})^2-2}{1+\dot{\zeta}} & \vdots & \dfrac{2}{1+\dot{\zeta}} \\ \cdots & \vdots & \cdots & \vdots & \cdots \\ 2 & \vdots & \dfrac{2}{1+\dot{\zeta}} & \vdots & \dfrac{(1+\dot{\zeta})^2-2}{1+\dot{\zeta}} \end{bmatrix}$$

$$= \begin{bmatrix} 0 & \vdots & \frac{1}{2} & \vdots & \frac{1}{2} \\ \cdots & \vdots & \cdots & \vdots & \cdots \\ \frac{1}{2} & \vdots & \frac{1}{4} & \vdots & \frac{1}{4} \\ \cdots & \vdots & \cdots & \vdots & \cdots \\ \frac{1}{2} & \vdots & \frac{1}{4} & \vdots & \frac{1}{4} \end{bmatrix} \tag{141}$$

$$[\dot{S}^B] = \begin{bmatrix} \dot{S}^B_{ll} & \vdots & \dot{S}^B_{lu} & \vdots & \dot{S}^B_{lr} \\ \cdots & \vdots & \cdots & \vdots & \cdots \\ \dot{S}^B_{ul} & \vdots & \dot{S}^B_{uu} & \vdots & \dot{S}^B_{ur} \\ \cdots & \vdots & \cdots & \vdots & \cdots \\ \dot{S}^B_{rl} & \vdots & \dot{S}^B_{ru} & \vdots & \dot{S}^B_{rr} \end{bmatrix} = \begin{bmatrix} 0 & \vdots & 0 & \vdots & \frac{1}{2} \\ \cdots & \vdots & \cdots & \vdots & \cdots \\ 0 & \vdots & 0 & \vdots & \frac{1}{2} \\ \cdots & \vdots & \cdots & \vdots & \cdots \\ \frac{1}{2} & \vdots & \frac{1}{2} & \vdots & 0 \end{bmatrix} \tag{142}$$

$$
[\dot{S}] = \begin{bmatrix}
0 & \dot{S}^{J}_{du}\dot{S}^{B}_{lu}\dot{S}^{F}_{lr}* & \dot{S}^{I}_{du}\dot{S}^{C}_{du}* & \dot{S}^{K}_{lr}\dot{S}^{B}_{lr}\dot{S}^{F}_{lr}* \\
 & *\dot{S}^{P}_{lr}\dot{S}^{H}_{lr} & *\dot{S}^{P}_{lu}\dot{S}^{H}_{lr} & *\dot{S}^{P}_{lr}\dot{S}^{H}_{lr} \\
\cdots & \cdots & \cdots & \cdots \\
\dot{S}^{H}_{rl}\dot{S}^{P}_{rl}\dot{S}^{F}_{rl}* & 0 & \dot{S}^{I}_{du}\dot{S}^{C}_{du}\dot{S}^{P}_{ru}* & \dot{S}^{K}_{lr}\dot{S}^{B}_{ur}\dot{S}^{J}_{ud}+ \\
*\dot{S}^{B}_{ul}\dot{S}^{J}_{ud} & & *\dot{S}^{F}_{rl}\dot{S}^{B}_{ur}\dot{S}^{J}_{ud} & +\dot{S}^{K}_{lr}\dot{S}^{B}_{lr}\dot{S}^{F}_{lr}* \\
 & & & *\dot{S}^{P}_{rr}\dot{S}^{F}_{rl}\dot{S}^{B}_{ul}\dot{S}^{J}_{ud} \\
\cdots & \cdots & \cdots & \cdots \\
\dot{S}^{H}_{rl}\dot{S}^{P}_{ul}* & \dot{S}^{J}_{du}\dot{S}^{B}_{lu}\dot{S}^{F}_{lr}* & \dot{S}^{I}_{du}\dot{S}^{C}_{du}\dot{S}^{P}_{uu} & \dot{S}^{K}_{lr}\dot{S}^{B}_{lr}\dot{S}^{F}_{lr} \\
*\dot{S}^{C}_{ud}\dot{S}^{I}_{ud} & *\dot{S}^{P}_{ur}\dot{S}^{C}_{ud}\dot{S}^{I}_{ud} & *\dot{S}^{C}_{ud}\dot{S}^{I}_{ud} & *\dot{S}^{P}_{ur}\dot{S}^{C}_{ud}\dot{S}^{I}_{ud} \\
\cdots & \cdots & \cdots & \cdots \\
\dot{S}^{H}_{rl}\dot{S}^{P}_{rl}\dot{S}^{F}_{rl}* & \dot{S}^{J}_{du}\dot{S}^{B}_{ru}\dot{S}^{K}_{rl} & \dot{S}^{I}_{du}\dot{S}^{C}_{du}\dot{S}^{P}_{ru}* & \dot{S}^{K}_{lr}\dot{S}^{B}_{lr}\dot{S}^{F}_{lr}* \\
*\dot{S}^{B}_{rl}\dot{S}^{K}_{rl} & & *\dot{S}^{F}_{lr}\dot{S}^{B}_{rl}\dot{S}^{K}_{rl} & *\dot{S}^{P}_{rr}\dot{S}^{F}_{rl}\dot{S}^{B}_{rl}\dot{S}^{K}_{rl}
\end{bmatrix} \tag{143}
$$

$$
[\dot{S}] = \begin{bmatrix}
0 & 0 & \frac{1}{8} & \frac{1}{4} \\
\cdots & \cdots & \cdots & \cdots \\
0 & 0 & 0 & \frac{1}{2} \\
\cdots & \cdots & \cdots & \cdots \\
\frac{1}{8} & 0 & \frac{1}{64} & \frac{1}{32} \\
\cdots & \cdots & \cdots & \cdots \\
\frac{1}{4} & \frac{1}{2} & \frac{1}{32} & \frac{1}{16}
\end{bmatrix} \tag{144}
$$

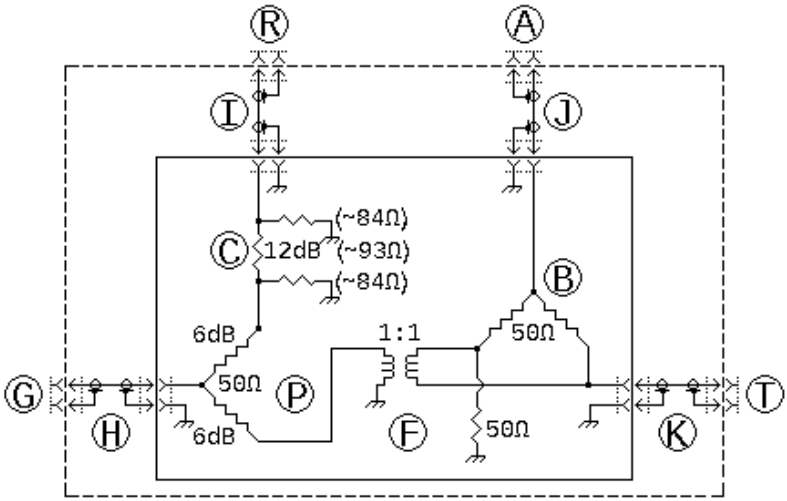

Fig. 7: Simplified T/R Test Set equivalent circuit

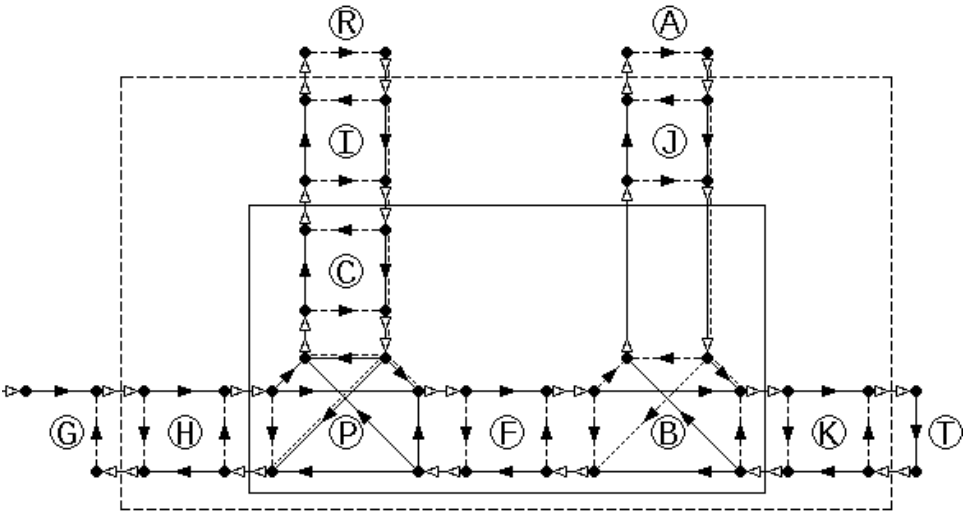

Fig. 8: Flow graph of the simplified T/R Test Set of Fig. 7

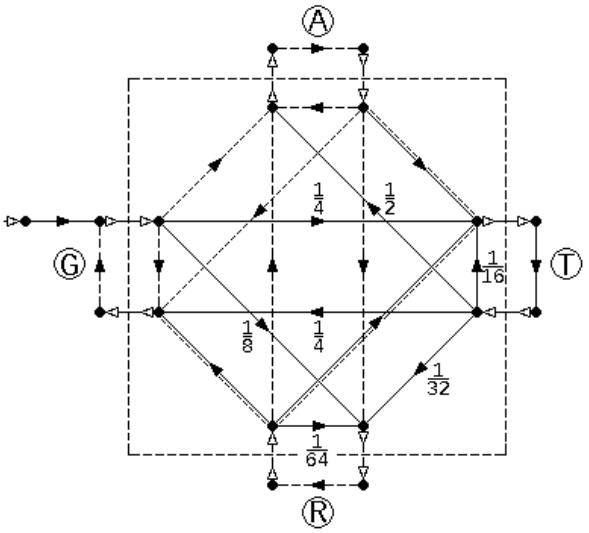

Fig. 9: The four port flow graph of the simplified IE

$$[\dot{S}] = \begin{bmatrix} 0 & 0 & \frac{1}{8}e^{-\dot{\gamma}^H L^H} e^{-\dot{\gamma}^I L^I} & \frac{1}{4}e^{-\dot{\gamma}^H L^H} e^{-\dot{\gamma}^K L^K} \\ \cdots & \cdots & \cdots & \cdots \\ 0 & 0 & 0 & \frac{1}{2}e^{-\dot{\gamma}^J L^J} e^{-\dot{\gamma}^K L^K} \\ \cdots & \cdots & \cdots & \cdots \\ \frac{1}{8}e^{-\dot{\gamma}^H L^H} e^{-\dot{\gamma}^I L^I} & 0 & \frac{1}{64}e^{-2\dot{\gamma}^I L^I} & \frac{1}{32}e^{-\dot{\gamma}^I L^I} e^{-\dot{\gamma}^K L^K} \\ \cdots & \cdots & \cdots & \cdots \\ \frac{1}{4}e^{-\dot{\gamma}^H L^H} e^{-\dot{\gamma}^K L^K} & \frac{1}{2}e^{-\dot{\gamma}^J L^J} e^{-\dot{\gamma}^K L^K} & \frac{1}{32}e^{-\dot{\gamma}^I L^I} e^{-\dot{\gamma}^K L^K} & \frac{1}{16}e^{-2\dot{\gamma}^K L^K} \end{bmatrix} \tag{146}$$

$$\frac{\dot{a}_A}{\dot{a}_R} = \frac{\dot{S}_{AG} + (\dot{S}_{AT}\dot{S}_{TG} - \dot{S}_{TT}\dot{S}_{AG})\dot{\rho}}{\dot{S}_{RG} + (\dot{S}_{RT}\dot{S}_{TG} - \dot{S}_{TT}\dot{S}_{RG})\dot{\rho}} = \tag{147}$$

$$= \frac{0 + \dot{S}_{AT}\dot{S}_{TG}\dot{\rho}}{\dot{S}_{RG} + 0\dot{\rho}} = \left(\frac{e^{-\dot{\gamma}^J L^J}}{e^{-\dot{\gamma}^I L^I}}\right) e^{-2\dot{\gamma}^K L^K}\dot{\rho} \qquad \text{And finally}$$

$$= \left(\frac{e^{-\dot{\gamma}^J L^J}}{e^{-\dot{\gamma}^I L^I}}\right) e^{-2\dot{\gamma}^K L^K}\dot{\rho}$$

$$\frac{\dot{a}_A}{\dot{a}_R} = e^{-2\dot{\gamma}^K L^K}\dot{\rho} \quad (148)$$

which concludes from the fact that the I, J transmission lines are identical in size and type.

A. Response Calibration

Response calibration means that instead of three Standard Loads we have only one available, the short circuit, which measurement is the reference for any other unknown load [29], [30]. As we mentioned before a typical value for this load is –1 and if for simplicity we assume that

$$\dot{\alpha}(f)\dot{\sigma} = 1 \quad (149)$$

then (148) becomes

$$\dot{s} = e^{-2\dot{\gamma}^K L^K}\dot{\rho} = e^{-2\dot{\gamma}^K L^K}\dot{S} = \\ = -e^{-2\dot{\gamma}^K L^K} \quad (150)$$

Thus, for an unknown load

$$\dot{m} = e^{-2\dot{\gamma}^K L^K}\dot{\rho} = -\dot{s}\dot{\rho} \Rightarrow \dot{\rho} = -\frac{\dot{m}}{\dot{s}} \quad (151)$$

B. A typical measurement application

First we assume that the three Standard loads $\dot{S}$, $\dot{L}$, $\dot{O}$, for the calibration procedure posses their theoretical values ([31], [32])

$$\dot{S} = -1.0,\ \dot{L} = 0.0,\ \dot{O} = 1.0 \quad (152)$$

Thus, the quantities of (130), (134) - (137) are simplified as

$$[\dot{A}] = \dot{o} - \dot{s} \quad (153)$$

$$\dot{Q} = \frac{\dot{l}(\dot{o} + \dot{s}) - 2\dot{o}\dot{s}}{\dot{o} - \dot{s}} \quad (154)$$

$$\dot{D} = \dot{l} \quad (155)$$

$$\dot{M} = \frac{\dot{o} + \dot{s} - 2\dot{l}}{\dot{o} - \dot{s}}g \quad (156)$$

$$\dot{R} = \frac{2(\dot{l} - \dot{o})(\dot{s} - \dot{l})}{\dot{o} - \dot{s}} \quad (157)$$

$$\boxed{\dot{\rho} = \frac{(\dot{m} - \dot{l})(\dot{o} - \dot{s})}{(\dot{m} - \dot{o})(\dot{s} - \dot{l}) - (\dot{m} - \dot{s})(\dot{l} - \dot{o})}} \quad (158)$$

the ρ-mini expression for the reflection coefficient [12], which can be written in the bilinear form (159)

$$\dot{\rho} = \frac{\dot{m}(\dot{o} - \dot{s}) + (-\dot{l}(\dot{o} - \dot{s}))}{\dot{m}(\dot{s} + \dot{o} - 2\dot{l}) + (\dot{l}(\dot{s} + \dot{o}) - 2\dot{s}\dot{o})}$$

In Fig.10 are illustrated the three error parameters $\dot{D}$, $\dot{M}$, $\dot{R}$ where they are given in plane as real, with single prime, and imaginary part with double prime and in space as functions of frequency for the range 550 MHz-1300 MHz. The VNA system used is fully described in [11] and [33] as the first system.

The automated measurements were taken by means of our program [ANALYZE] through HPIB/IEEE 488 [34].

Then we measured one of the 436 antenna models that were constructed [35] with the geometric model of Fig. 11, which is one of the four possible arrangements of a multi-frequency decoupling cylinder with one of the possible monopoles, here the conical one. Fig. 12 shows the simulation model with 16 wires for the cylinders and 8 wires for the conical monopole with dimensions: $d_1 = 8cm$, $L_1 = 9cm$, $d_2 = .9.6cm$ $L_2 = 8cm$, $s = = 0.8cm$, $\alpha = = 90°$, $H = 6cm$. Full details of the construction are given in [35].

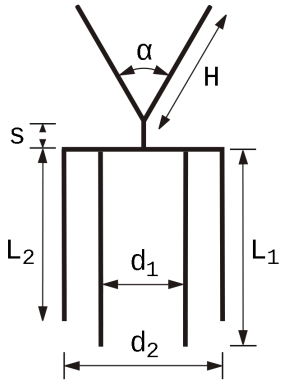

Fig. 11 Antenna geometry with down external step

The antenna's reflection coefficient after full one-port calibration with SLO (158) and after only response calibration S (151) is shown in plane and in space as function of frequency in Fig. 13 among with their comparison. In Fig. 14 the antenna's input impedance is illustrated as real and imaginary part together with their prediction from simulation by [RICHWIRE] [36], with the gray cloud to represent their measurements' DEIs (Differential Error Intervals) [11]. All the measurements were performed in the anechoic chamber of the Antennas Research Group when it was hosted by the university.

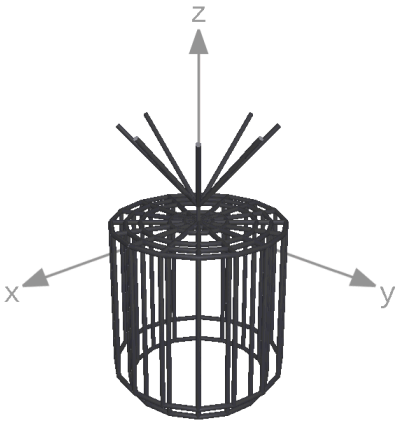

Fig. 12: Simulation model

The input impedance is given by the well known expression as function of $\dot{\rho}$

$$\dot{Z} = Z_0 \frac{1 + \dot{\rho}}{1 - \dot{\rho}} \qquad (160)$$

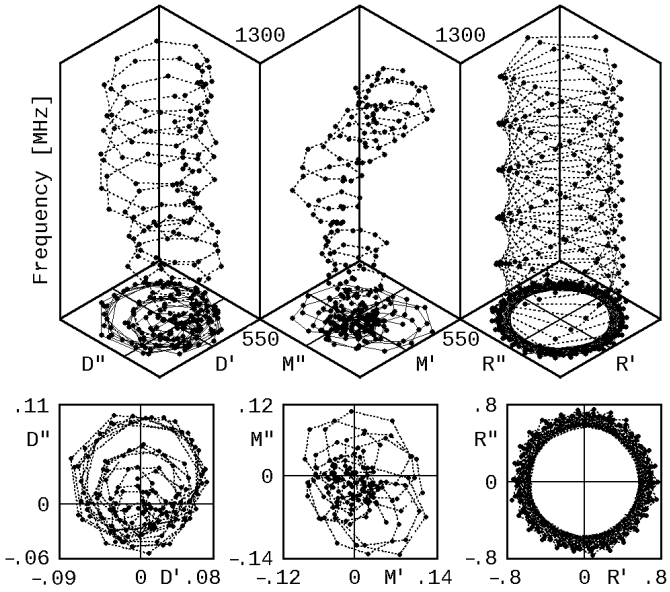

Fig. 10: D, M, R as function of frequency

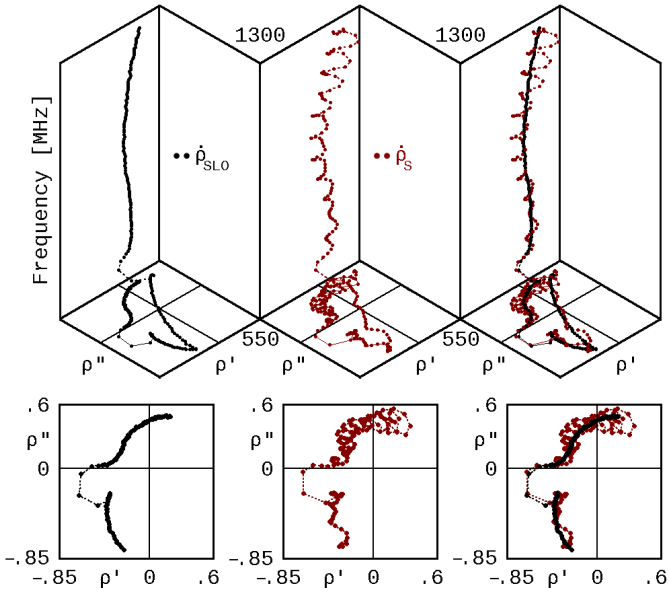

Fig. 13: Antenna’s reflection coefficient

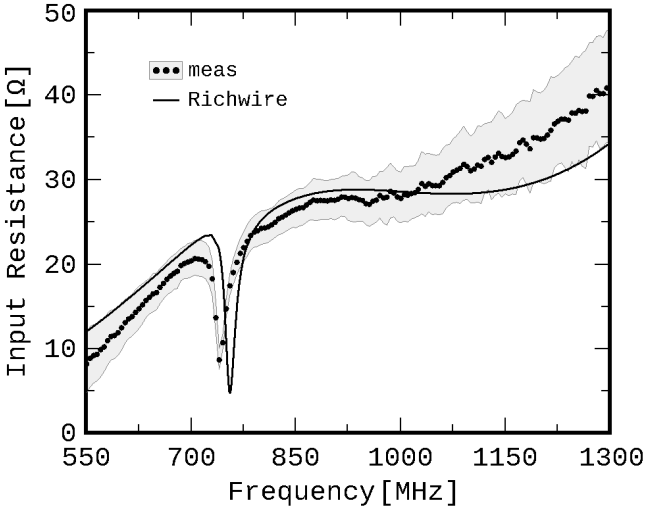

Input impedance real part

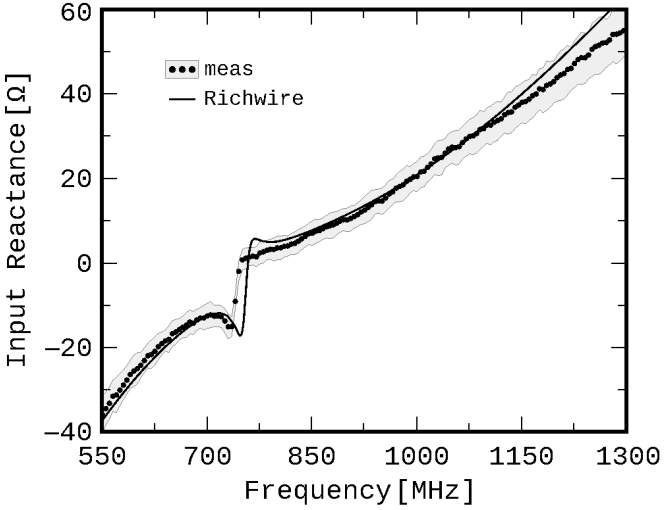

Input impedance imaginary part

Fig. 14: Antenna’s input impedance

or by substitution of $\dot{\rho}$ from ρ-mini (158)

$$\dot{Z} = -Z_0 \frac{(\dot{m} - \dot{s})(\dot{l} - \dot{o})}{(\dot{m} - \dot{o})(\dot{s} - \dot{l})} \quad (161)$$

and as bilinear form

$$\dot{Z} = -Z_0 \frac{\dot{m}(\dot{l} - \dot{o}) + (-\dot{s}(\dot{l} - \dot{o}))}{\dot{m}(\dot{s} - \dot{l}) + (-\dot{o}(\dot{s} - \dot{l}))} \quad (162)$$

Conclusions

This work presented a conceptual model for the reflection measurements of a VNA System. The sets of values of all involved quantities and their corresponding functions, that define the relations between them, are produced in detail.

The transition, from the four-port microwave junction, that represents the measuring operation of a VNA System for reflection measurements, to the reflection full one-port error model, was completely revealed.

The frequency dependent systematic error parameters were expressed, computed, and drawn.

A constructed antenna with a rather complex geometry having cylindrical symmetry was measured and the results for its reflection coefficient $\dot{\rho}$, as well as its directly dependent on $\dot{Z}$ input impedance, were presented.

Finally, although the Lab VNA System includes an externally "Inserted Equipment" IE (that obviously serves the clever ensemble of VNA Systems having a variety of characteristic impedance and connectors, e.g. as it is shown in the simplified T/R Set circuit of Fig. 7, where only the bridge B and its branches need to be changed to 75Ω, while the whole of the other System remains exactly the same 50Ω [37]), its reflection full one-port error model is identical to that of a NanoVNA, where although the IE appears to be a missing component, but in fact it is an internally included device - the full details will be included in a forthcoming paper.

References – Updates – MD5 check

https://www.ftpj.otoiser.org/refs/392.htm

[1] HP, "Vector Measurements of High Frequency Networks", HP publication number 5958-0387, 1989, pp. 3-2 - 3-9

https://ftpj.otoiser.org/refs/392.htm#r1

archive.org/details/vector-measurements-of-high-frequency-networks-paul-schmitz-april-1989-hp-5958-0387

[2] Bianco B., Corana A., Ridella S., Simicich C., "Evaluation of Errors in Calibration Procedures for Measurements of Reflection Coefficient", IEEE Transactions of Instrumentation and Measurement", Vol. IM-27, No. 4, 1978 pp. 354 - 359

[3] Fitzpatrick J., "Error Models for Systems Measurement", Microwave Journal, May 1978, pp. 63 - 66

[4] Young P. R., "Propagation of uncertainty in one-port ANA measurements", ANAMET Report 017, August 1998

[5] Eul H.-J., Schiek B., "A Generalised Theory and New Calibration Procedures for Network Analyser Self-Calibration", IEEE Transactions on Microwave Theory and Techniques, Vol. 39, No. 4, 1991, pp. 724 - 731

[6] Soares R. A., Gouzien P., Legaud P., Follot G., "A Unified Mathematical Approach to Two-Port Calibration Techniques and Some Applications", Transactions on Microwave Theory and Techniques, Vol. 37, No. 11, 1989, pp. 1669 - 1673

[7] "Reference Data for Radio Engineers", Howard W. Sams & Co - ITT, "Ch. 24: Scattering Matrices", 5th Ed., 1972, pp. 1 - 9

[8] Spiegel M. R., "Complex Variables with an introduction to Conformal Mapping and its applications", McGraw-Hill, 1974, pp. 34, 203

[9] Chipman R. A., "Transmission Lines", McGraw Hill, 1968, Ch. 7, pp. 126 - 155

[10] Yannopoulou N. I., Zimourtopoulos P. E., "Measurement Uncertainty in Network Analyzers: Differential Error Analysis of Error Models Part 1: Full One-Port Calibration", FunkTechnikPlus # Journal, Issue 1, Year 1, 2013, pp. 17 - 22

https://ftpj.otoiser.org/refs/392.htm#r10

ftpj.otoiser.org/issues/html/ftpj-issue-01-e4-lo4104-pdfc171-ia1.htm#r12 (1-2)

[11] Yannopoulou N., Zimourtopoulos P., "Total Differential Errors in One-Port Network Analyzer Measurements with Application to Antenna Impedance", Radioengineering, Vol. 16, No. 2, June 2007, pp. 1 - 8

https://ftpj.otoiser.org/refs/392.htm#r11

radioeng.cz/fulltexts/2008/08_01_01_08.pdf

[12] Yannopoulou N. I., Zimourtopoulos P. E., "Comparing a NanoVNA with a LabVNA Part 1: One-Port Measurements", FunkTechnikPlus # Journal, Issue 34, Year 11, 2024, pp. 7 - 41

https://ftpj.otoiser.org/refs/392.htm#r12

ftpj.otoiser.org/issues/html/ftpj-issue-34-lo7532-export-ia1.htm#r341 (34-1)

[13] HP, "8660C Synthesized Signal Generator", HP Operating and Service Manual, May 1979

[14] HP, "86603 RF Section 1-2600MHz", HP Operating and Service Manual, October 1978

[15] HP, "5340 Frequency Counter", HP Operating and Service Manual, September 1975

[16] HP, "8505A Network Analyzer: Operating and Programming", HP Operating and Service Manual, Vol. 1 - A3, Santa Rosa California, USA, August 1979

[17] HP, "8505A Network Analyzer Option 005 Phase Lock", HP Option Supplement Vol. 3 - Chapter E, August 1979

[18] HP, "Using the HP-IB Interface with MS Windows", 1991

[19] HP, "Calculator Control of the 8660A/B/C Synthesized signal generator", HP Application Note 164-2, Aug. 1979

[20] "MS Visual Basic Programming System for Windows v.3.0 (in three books)", Microsoft, 1993

[21] Wolfram Stephen, "The Mathematica Book", Wolfram Research, 1996

[22] Wagner D. B., "Power Programming with Mathematica: The Kernel", McGraw-Hill, 1996

[23] HP, "HP 8505A RF Network Analyzer Basic Measurements", Application Note 219, Palo Alto California, November 1978

https://ftpj.otoiser.org/refs/392.htm#r23

www.hpmemoryproject.org/an/pdf/an_219.pdf

[24] HP, "High Performance RF Network Analyzer", "8505A Specifications", Technical Data, 5952-9268, Palo Alto California, January 1979, pp. 14 - 15

https://ftpj.otoiser.org/refs/392.htm#r24

archive.org/details/high-performance-rf-network-analyzer-hp-8505-a

[25] HP, "8505A Network Analyzer HP Operating and Service Manual", Vol. 1, A1-5 - A1-7, A3-28, A4, August 1979

[26] HP, "8502A Transmission/Reflection Test Set", HP Operating and Service Manual, October 1979

https://ftpj.otoiser.org/refs/392.htm#r26

keysight.com/dk/en/assets/9018-02748/user-manuals/9018-02748.pdf

[27] Kuhn N., "Simplified signal flow graph analysis", Microwave Journal, November 1963, pp. 59 - 66

[28] Collin R. E., "Foundations for Microwave Engineering", John Wiley & Sons Inc., 2nd Ed., 2001, pp. 260 - 268

[29] Keysight, "OPEN/SHORT Response Calibration (reflection test)"

https://ftpj.otoiser.org/refs/392.htm#r29

helpfiles.keysight.com/csg/e5071c/measurement/calibration/basic_calibrations/open_short_response_calibration_reflection_test.htm

[30] Keysight, "Calibration Types and Characteristics"

https://ftpj.otoiser.org/refs/392.htm#r30

helpfiles.keysight.com/csg/e5071c/measurement/calibration/calibration_types_and_characteristics.htm

[31] Keysight Technologies Inc., "909A Coaxial Termination DC to 18 GHz"

https://ftpj.otoiser.org/refs/392.htm#r31

keysight.com/dk/en/assets/7018-03039/technical-overviews/5990-8462.pdf

[32] Maury Microwave, "Precision Microwave Instruments and Components", 1996, p. 132

[33] Yannopoulou N. I., Zimourtopoulos P. E., "Various Loads as Calibration Standards for Vector Network Analyzer Measurements" FunkTechnikPlus # Journal, Issue 38, Year 13, 2025, pp. 13 - 42

https://ftpj.otoiser.org/refs/392.htm#r33

ftpj.otoiser.org/issues/html/ftpjissue38lo7532exportia1.htm#r382 (38-2)

[34] Yannopoulou N., Zimourtopoulos P., "ANALYZE: Automated Antenna Measurements, ver. 13", Antennas Research Group, 1993 - 2008

[35] Yannopoulou N. I., "Study of monopole antennas over a multi-frequency decoupling cylinder", PhD Thesis, EECE, DUTh, February 2008 (in Hellenic), pp. 3-27, 5-175 - 5-177

https://ftpj.otoiser.org/refs/392.htm#r35

www.didaktorika.gr/eadd/handle/10442/20920?locale=en

[36] Richmond J. H., "Computer program for thin-wire structures in a homogeneous conducting medium", Publication Year: 1974, NTRS-Report/Patent Number: NASA-CR-2399, ESL-2902-12, DocumentID: 19740020595

https://ftpj.otoiser.org/refs/392.htm#r36

ntrs.nasa.gov/search.jsp?R=19740020595

[37] HP, "8502B 75-Ω Transmission/Reflection Test Set", HP Operating and Service Manual, March 1977

https://ftpj.otoiser.org/refs/392.htm#r37

keysight.com/dk/en/assets/9018-03263/user-manuals/9018-03263.pdf